

RESEARCH ARTICLE

Electronic properties of monolayer copper selenide with one-dimensional moiré patterns

Gefei Niu^{1,*}, Jianchen Lu^{1,*†}, Jianqun Geng^{1,*}, Shicheng Li¹, Hui Zhang¹, Wei Xiong¹, Zilin Ruan¹, Yong Zhang¹, Boyu Fu¹, Lei Gao^{2,‡}, Jinming Cai^{1,#}

¹Faculty of Materials Science and Engineering, Kunming University of Science and Technology, Kunming 650093, China

²Faculty of Science, Kunming University of Science and Technology, Kunming 650500, China

*These authors contributed equally.

Corresponding authors. E-mail: [†]jclu@kust.edu.cn, [‡]lgao@kust.edu.cn, [#]j.cai@kust.edu.cn

Received June 7, 2022; accepted October 11, 2022

Supporting Information

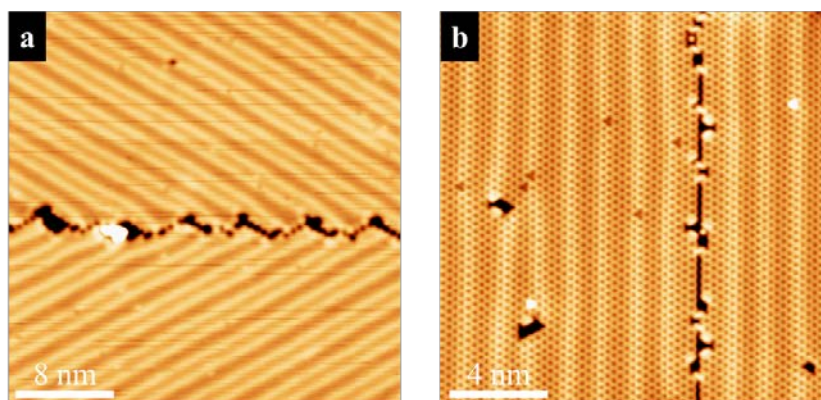


Fig. S1 Morphology of line-defect formed by mirror-symmetric domains. **(a)** A large-scale STM image of the folding line-defect. **(b)** A large-scale STM image of the straight line-defect. Scanning parameters: (a) $V_s = 2$ V, $I_t = 50$ pA; (b) $V_s = 0.2$ V, $I_t = 100$ pA.

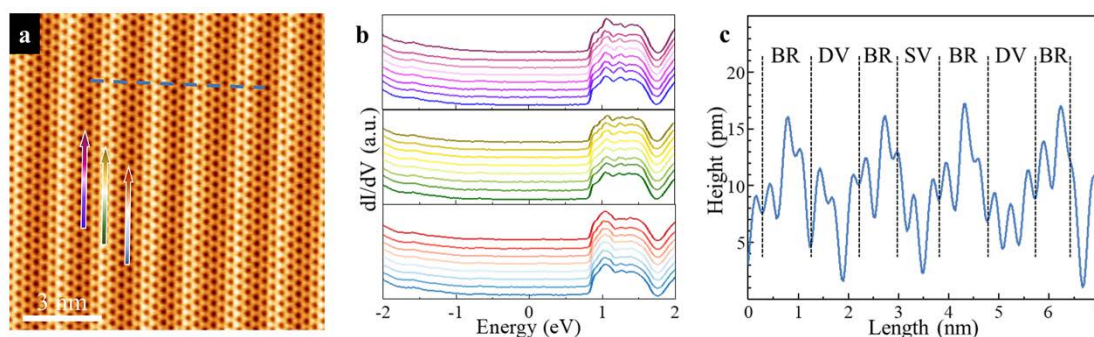


Fig. S2 Electronic properties of 1D moiré patterns of CuSe monolayer. **(a)** An atomic-resolved STM image of 1D moiré patterns of CuSe monolayer with hexagonal honeycomb lattice. **(b)** Three waterfall plots of dI/dV curves along the gradient arrows in (a). **(c)** Line-profile perpendicular to 1D moiré patterns, indicated by a blue dashed line in (a), showing three distinct regions. Scanning parameters: (a) $V_s = -0.42$ V, $I_t = 300$ pA; (b) $V_s = 1.5$ V, $I_t = 400$ pA, $V_{rms} = 10$ mV.

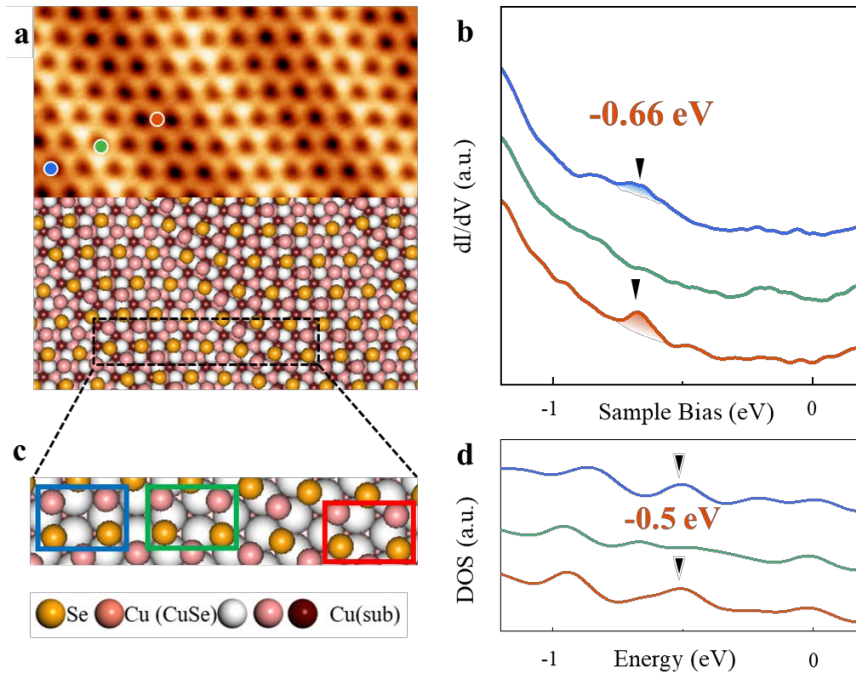


Fig. S3 Structural and electronic properties of monolayer CuSe on Cu(111). **(a)** An atomically resolved STM image and corresponding optimized atomic structure of monolayer CuSe on Cu(111). **(b)** Three dI/dV curves collected at different positions which are marked by blue, green and red dots in (a). **(c)** Zoom-in atomic structure from a black square in (a). **(d)** Projected density of states (PDOSs) contributed by in-plane orbitals (Se p_x/p_y and Cu $d_{xy}/d_{x^2-y^2}/d_z^2$) calculated at different positions which are marked by blue, green and red squares in (c).

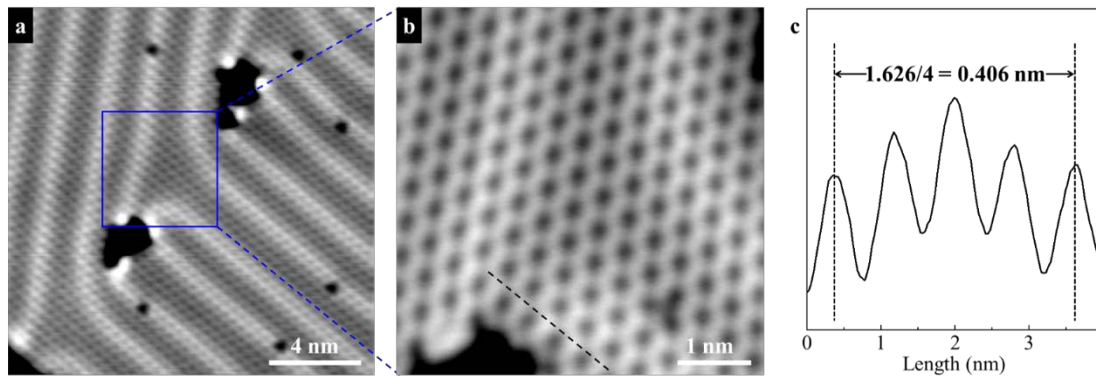


Fig. S4 Domain boundaries of CuSe monolayer with 1D moiré patterns. **(a)** A large scale STM image of domain boundary of CuSe monolayer. **(b)** A zoom-in atomically resolved STM image of domain boundary, showing a continuous CuSe honeycomb lattice. **(c)** The line-profiles perpendicular to continuous boundary of 1D moiré patterns structure of CuSe, indicated by the black line in (b). Scanning parameters: (a) $V_s = 50$ mV, $I_t = 100$ pA; (b) $V_s = 10$ mV, $I_t = 500$ pA.

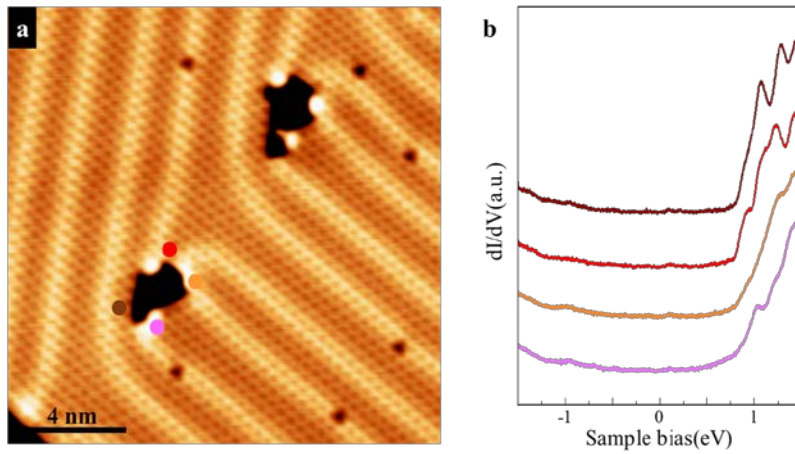


Fig. S5 The electronic properties around the defect of continuous boundaries. **(a)** A large scale STM image of continuous boundary of CuSe monolayer with hexagonal honeycomb lattice. **(b)** dI/dV curves collected at four positions, as indicated by colored dots in (a). Scanning parameters: (a) $V_s = 50$ mV, $I_t = 1.3$ nA; (b) $V_s = 2$ V, $I_t = 300$ pA, $V_{rms} = 10$ mV.

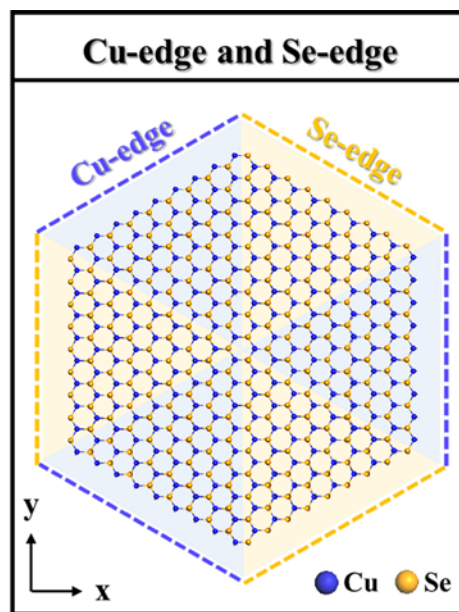


Fig. S6 Schematic model of edge terminations of an hexagonal CuSe island, where the Cu edge and Se edge are illustrated by blue and yellow dashed lines, respectively.

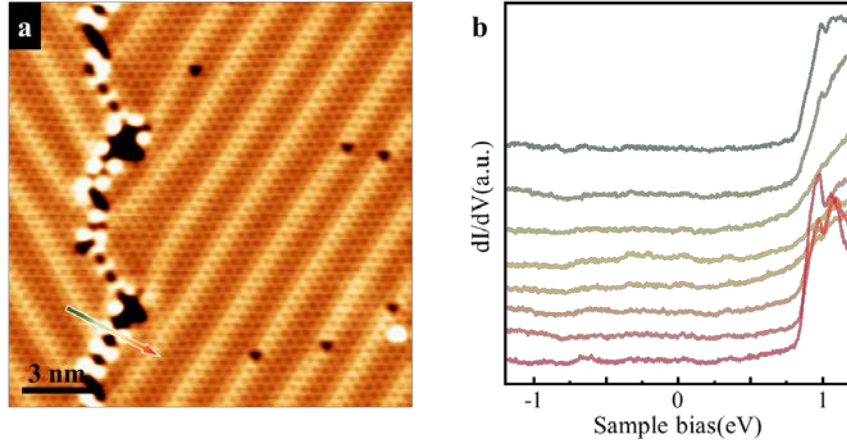


Fig. S7 The electronic properties crossing the line-defect formed by mirror-symmetric domains. **(a)** A large-scale STM image of the line-defect. **(b)** The waterfall plot of the dI/dV curves along the gradient arrows in (a). Scanning parameters: (a) $V_s = 0.4$ V, $I_t = 200$ pA; (b) $V_s = 2$ V, $I_t = 400$ pA, $V_{rms} = 10$ mV.

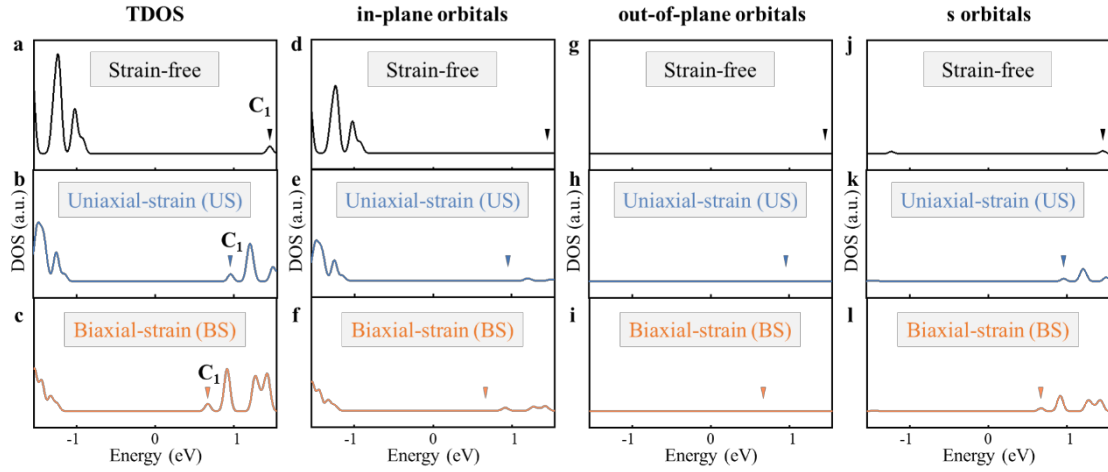


Fig. S8 Calculated PDOSs of monolayer CuSe under strain-free, 7.3% uniaxial-strain and 7.3% biaxial-strain on Cu(111). **(a-c)** Total density of states (TDOSs). **(d-f)** PDOSs contributed by in-plane orbitals (Se p_x/p_y and Cu $d_{xy}/d_{x^2-y^2}/d_z^2$). **(g-i)** PDOSs contributed by out-of-plane orbitals (Se p_z and Cu d_{xz}/d_{yz}). **(j-l)** PDOSs contributed by s orbitals of Cu and Se atoms.